

A Scaled Smart City for Experimental Validation of Connected and Automated Vehicles ^{*}

Adam Stager ^{*} Luke Bhan ^{**} Andreas Malikopoulos ^{*}
Liuhui Zhao ^{*}

^{*} *University of Delaware, Newark, DE 19716 USA (e-mails: astager@udel.edu; andreas@udel.edu; lzhao@udel.edu).*

^{**} *Avon Grove High School, West Grove, PA 19390 USA (e-mail: lukebhan@udel.edu)*

Abstract: The common thread that characterizes energy efficient mobility systems for smart cities is their interconnectivity which enables the exchange of massive amounts of data; this, in turn, provides the opportunity to develop a decentralized framework to process this information and deliver real-time control actions that optimize energy consumption and other associated benefits. To seize these opportunities, this paper describes the development of a scaled smart city providing a glimpse that bridges the gap between simulation and full scale implementation of energy efficient mobility systems. Using this testbed, we can quickly, safely, and affordably experimentally validate control concepts aimed at enhancing our understanding of the implications of next generation mobility systems.

Keywords: Smart cities, connected and automated vehicles, vehicle coordination, cooperative merging control.

1. INTRODUCTION

In a rapidly urbanizing world, we need to make fundamental transformations in how we use and access transportation. Energy efficient mobility systems such as Connected and Automated Vehicles (CAVs) along with shared mobility and electric vehicles provide the most intriguing and promising opportunities for enabling users to better monitor transportation network conditions and make better operating decisions to reduce energy consumption, greenhouse gas emissions, travel delays and improve safety. As we move to increasingly complex transportation systems new control approaches are needed to optimize the system behavior resulting from the interactions between vehicles navigating different traffic scenarios.

Given this new environment, the overarching goal of this paper is to report on the development of the University of Delaware Scaled Smart City (UDSSC) that includes 35 robotic cars to replicate real-world traffic scenarios in a small and controlled ecosystem. UDSSC can serve as a testbed to explore the acquisition and processing of vehicle-to-vehicle and vehicle-to-infrastructure communication. It can also help us prove control concepts on coordinating CAVs in specific transportation scenarios, e.g., intersections, merging roadways, roundabouts, speed reduction zones, etc. These scenarios along with the driver responses to various disturbances are the primary sources of bottlenecks that contribute to traffic congestion; see Malikopoulos and Aguilar (2013); Margiotta and Snyder (2011). In 2015, congestion caused people in urban areas

in the US to spend 6.9 billion additional hours on the road and to purchase an extra 3.1 billion gallons of fuel, resulting in a total cost estimated at \$160 billion; see (Schrank et al., 2015).

CAVs can provide shorter gaps between vehicles and faster responses while improving highway capacity. Several research efforts have been reported in the literature proposing either *centralized* or *decentralized* approaches for coordinating CAVs in specific traffic scenarios. The overarching goal of such efforts is to yield a smooth traffic flow avoiding stop-and-go driving. Numerous approaches have been reported in the literature on coordinating CAVs in different transportation scenarios with the intention of improving traffic flow. Kachroo and Li (1997) proposed a longitudinal and lateral controller to guide the vehicle until the merging maneuver is completed. Other efforts have focused on developing a hybrid control aimed at keeping a safe headway between vehicles in the merging process, see Antoniotti et al. (1997); Kachroo and Li (1997); or developing three levels of assistance for the merging process to select a safe space for the vehicle to merge; see Ran et al. (1999). Some authors have explored virtual vehicle platooning for autonomous merging control, e.g., Dresner and Stone (2004); Lu et al. (2000), where a controller identifies and interchanges appropriate information between the vehicles involved in the merging maneuver while each vehicle assumes its own control actions to satisfy the assigned time and reference speed.

VanMiddlesworth et al. (2008) addressed the problem of traffic coordination for small intersections which commonly handle low traffic loads. Milanés et al. (2010) de-

^{*} This research was supported by the University of Delaware.



Fig. 1. Birdseye view of the University of Delaware’s Scaled Smart City.

signed a controller that allows a fully automated vehicle to yield to an incoming vehicle in the conflicting road or to cross, if it is feasible without the risk of potential collision. Alonso et al. (2011) proposed two conflict resolution schemes in which an autonomous vehicle could make a decision about the appropriate crossing schedule and trajectory to follow to avoid collision with other manually driven vehicles on the road. A survey of the research efforts in this area that have been reported in the literature to date can be found in Rios-Torres and Malikopoulos (2017a).

Although previous work has shown promising results emphasizing the potential benefits of coordination between CAVs, validation has been primarily in simulation. In this paper, we demonstrate coordination of scaled CAVs and quantify the benefits in energy usage. The contributions of this paper are: 1) the development of a 1:24 scaled smart city capable of testing coordination control algorithms on up to 35 Micro Connected and Automated Vehicles (MCAVs) and 2) the experimental validation of a control framework reported in Rios-Torres and Malikopoulos (2017b) for coordination of CAVs.

The remainder of the paper proceeds as follows. In Section II, we introduce the configurations of UDSSC. In Section III, we review a decentralized control framework for coordination of CAVs in merging roadways. Experimental results in Section IV illustrate the effectiveness of the proposed solution in the scaled smart city environment. We draw concluding remarks in Section V.

2. UNIVERSITY OF DELAWARE SCALED SMART CITY (UDSSC)

UDSSC is a testbed that can replicate real-world traffic scenarios in a small and controlled environment and help us formulate the appropriate features of a “smart” city. It can be used as an effective way to visualize the concepts developed using CAVs and their related implications in energy usage. UDSSC is a fully integrated smart city (Fig. 1) incorporating realistic environmental cues, scaled MCAVs, and state-of-the-art, high-end computers supporting standard software for system analysis and optimization for simulating different control strategies and distributing control inputs to as many as 35 autonomous vehicles.

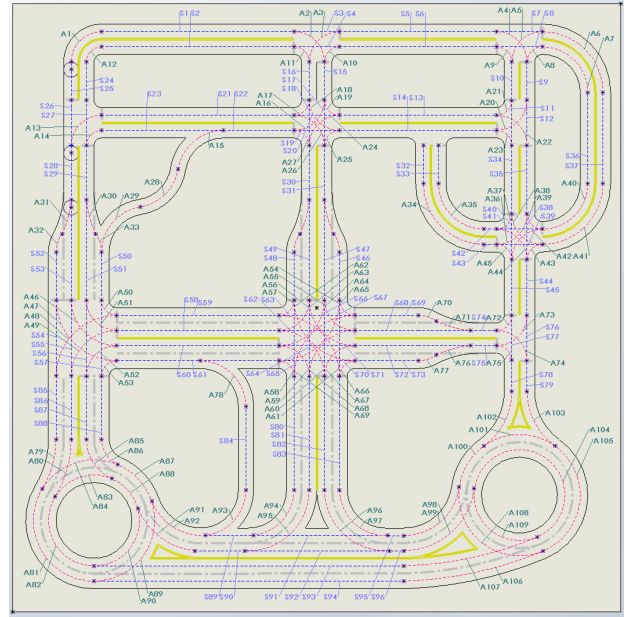


Fig. 2. SolidWorks provides a convenient workspace for representing fully dimensioned roadways including labeling for easy identification of each road segment.

2.1 Physical Design I: Map

The UDSSC spans over 400 square feet and includes one lane intersections, two lane intersections, roundabouts, and a highway with entrance and exit ramps. Using SolidWorks to accurately maintain 1:24 scale, a fully dimensioned two-dimensional blueprint (Fig. 2) was designed forming a cohesive roadway representative of real world road scenarios. Labels act as unique identifiers distinguishing between straight line and arc segments and containing path parameters. The blueprint is then exported into Adobe Illustrator where seamless texturing and environmental cues are added for realism. Special care has been taken to include three-dimensional aspects including, trees, houses and even humans so future work focusing on lane tracking will include realistic visual tracking elements. Using a HP DesignJet z5200 photo printer the entire layout is printed on twelve 44”x120” sheets of wear resistant HP Artist Matte Canvas that can be easily replaced to either reconfigure or repair sections of the city independently. Double sided carpet tape holds each map section to over 120 2’x2’x7/8” DRICore sub-floor panels helping to distribute floor level variations while providing a smooth mounting surface. Eight Vicon Vantage V16 cameras are used to localize the map within a globally recognized coordinate system. Critically, Vicon markers are placed atop each map subsection to locate a centralized origin and abate the effect of slight offsets and stretching in the canvas material. Once a map frame is initialized the dimensions of the road sections are known exactly and are easily referenced using the original two-dimensional blueprints.

2.2 Physical Design II: Cars

Scaled MCAVs have been designed using easily assembled off-the-shelf components coupled with several 3D printed parts (Fig. 3). At the core of each platform is a 75.81:1

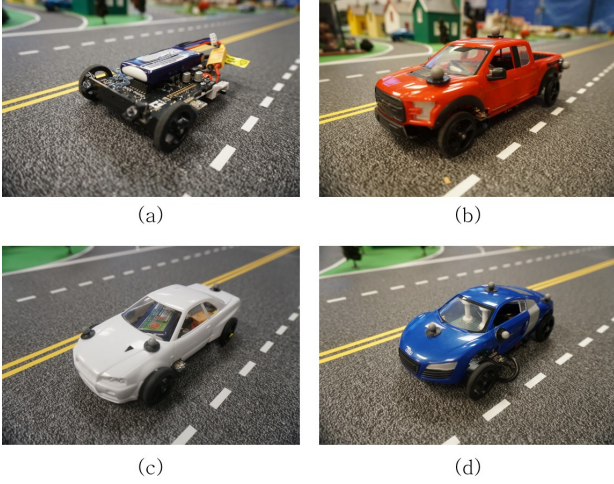


Fig. 3. The UDSSC incorporates 35 automated vehicles, each starting with the same MCAVs hardware (a) and incorporating different types of scaled vehicle shells such as a Ford F150 (b), Nissan Skyline (c), and Audi R8 (d).

geared, differentially driven Pololu Zumo, offering dual H-bridge motor drivers, $n_e = 12$ counts per revolution (CPR) encoders and an on-board Atmega 32U4 micro-controller. Additionally the Zumo contains an embedded set of sensors including a buzzer, IMU, line-following and infrared proximity sensors which can provide feedback to each MCAV. Although each Zumo is originally equipped with tracks, they are replaced with rubberized wheels with radius $r = 1.6$ cm mounted directly to each gear motor output shaft and separated by $d = 9$ cm to roughly mimic the 1:24 scale width of full sized cars/trucks. The MCAV platform (not including its car-shaped shell) measures 13 cm x 10.5 cm x 4.5 cm ($l/w/h$), keeping a low profile by replacing the traditional caster with a low-friction metal ball. The Pololu Zumo is connected to an on-board Raspberry Pi 3 with 1.2 GHz quad-core ARM Cortex A53 micro-processor and 2.4GHz 802.11n WiFi used for communication. It is worthwhile to note that this choice of micro-processor is not necessary for our currently implementation, but has been added to account for on-board processing envisioned for future experiments. A power regulator manages the voltage requirements of the Raspberry Pi 3, supplying a regulated 5VDC from a 7.4VDC, 1000mAh Li-Po battery. Fully charged MCAVs are capable of running approximately 90 minutes before being recharged at 6.8VDC.

In place of car-like models which would require a more complex mechanical design, Zumo based MCAVs are differentially driven and can be considered as a non-holonomic unicycle such with a vector of two control inputs, $u = [v, \omega]$, where v is the longitudinal speed and ω the angular velocity. Three state variables fully define the robot operating on a planar \mathbb{R}^2 workspace, with two states for position $(x, y) \in \mathbb{R}^2$ and a third for orientation, $\theta \in S^1$ designating the heading of the MCAV. The state space can therefore be defined as $X = \mathbb{R}^2 \times S^1$. The dynamics of each vehicle are

$$\dot{x}(t) = v \cos \theta, \quad \dot{y}(t) = v \sin \theta, \quad \dot{\theta}(t) = \omega. \quad (1)$$

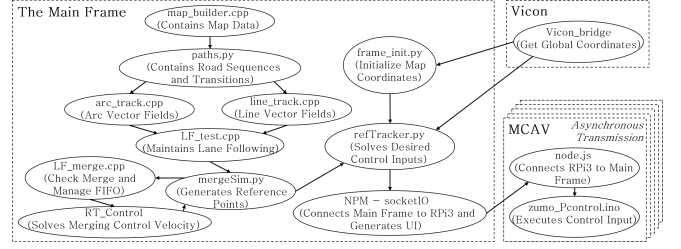


Fig. 4. Vicon Motion Tracking is combined with a multi-level control architecture making up the core of UDSSC.

Control inputs sent wirelessly to each vehicle are converted on-board into right and left wheel velocities maintained by each MCAV using encoder feedback.

2.3 Control System Architecture

UDSSC has a multi-level control architecture (see Fig. 4) with high level commands originating from a centralized PC called the “Main Frame” (Processor: Intel Core i7-6950X CPU @ 3.00 GHz x 20, Memory: 125.8 GiB) then enforced by a low-level controller on-board each MCAV. Asynchronous communication is enabled by WiFi connectivity using the Node.js non-blocking I/O protocol. Electron uses a socket server with a socketIO library natively supporting multi-threading for multi-vehicle communication. A web browser combines JavaScript, HTML, and CSS for a user friendly interface into the Robot Operating System (ROS) architecture. Generally control of each MCAV can be broken into merging, lane and reference tracking controllers, the latter two of which enforce realistic road behaviors (i.e. staying in the center of the road and respecting speed limits.)

Lane tracking: The roads of UDSSC are encoded as sequences of tangent arcs and straight line segments. A general representation of each of these road types is then encoded as a potential field directing a particle placed within from one end of the road to the other. Potential field methods not only allow for flexibility in the initial condition, but also provide important computational expedience due to their analytical representation. Given a looping sequence of road segments an MCAV can be placed anywhere on the first segment and will follow along the road until its battery is depleted.

Straight line roads can be described by,

$$\begin{aligned} \dot{x} &= dX + p(x_o - x - ((x_o - x)dX + (y_o - y)dY)dX) \\ \dot{y} &= dY + p(y_o - y - ((x_o - x)dX + (y_o - y)dY)dY), \end{aligned}$$

where (x_o, y_o) is the initial point, $[dX, dY]$ is a unit vector in the direction of the road and p is a tuning parameter such that larger values cause more dramatic convergence and overshoot. A length and width are also specified creating a region in which the vector field is active.

Arcs are described by,

$$\begin{aligned} \dot{x} &= r(y - y_c)cw - 4p(x - x_c)((x - x_c)^2 + (y - y_c)^2 - r^2) \\ \dot{y} &= -r(x - x_c)cw - 4p(y - y_c)((x - x_c)^2 + (y - y_c)^2 - r^2), \end{aligned}$$

where (x_c, y_c) designate the center of the arc and r the radius. Similarly to the straight line equation, a tuning

parameter drives faster convergence at higher values. A parameter $cw = 1$ if the rotational direction is clock-wise, otherwise $cw = -1$.

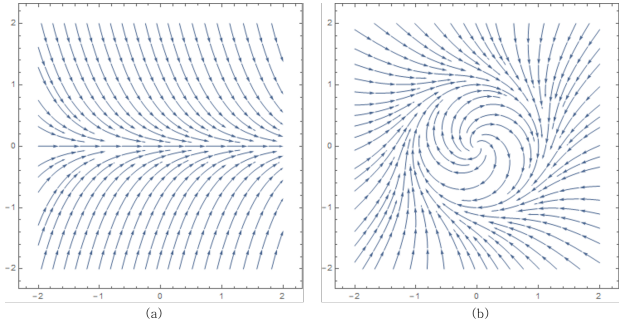


Fig. 5. Line (a) and arc (b) vector fields with parameter $p=2.0$ and $p=0.2$ respectively.

Transition regions are constructed by specifying half-planes at the intersection point between two road segments such that transition from the center of one road places a reference point in the center of the next. Although an MCAV can use lane tracking directly to follow along a road, while in the control region merging requires a carefully maintained forward velocity profile with respect to the lane center. Offsets from the centerline of the lane using lane tracking results in noisy forward velocity measurements, however a virtual robot can track the center of each lane exactly. For situations where more careful velocity profiles are required, such as in merging control, instead of controlling each MCAV using the potential field directly a virtual robot is simulated within the vector field and used as a reference point that is tracked by the real robot.

Reference tracking: As long as a reference point tracks a sequence of road segments using lane tracking the MCAV can be controlled by reference tracking. Knowing each MCAV is differentially driven a virtual robot with the same unicycle dynamics can be used for tracking with inputs $u = [v, \omega]$. A simple state tracking method as described in Giuseppe and Vendittelli (2002) is used (2), approximately linearizing the error dynamics of the MCAV's local frame with respect to a reference trajectory. Based on the original control input we can write,

$$\begin{aligned} v &= v_d \cos(\theta_d - \theta) + k_1((x_d - x) \cos(\theta) + (y_d - y) \sin(\theta)) \\ w &= w_d + k_2 \text{sign}(v_d)((y_d - y) \cos(\theta) - (x_d - x) \sin(\theta)) \\ &\quad + k_3(\theta_d - \theta), \end{aligned} \quad (2)$$

where v_d, ω_d, θ_d , given by the reference trajectory, are the desired velocity, angular velocity and orientation respectively. The gains of the controller k_1, k_2, k_3 , are chosen as in Giuseppe and Vendittelli (2002),

$$k_1 = k_2 = 2\zeta\sqrt{\omega_d^2(t) + bv_d^2(t)}, \quad k_3 = bv_d(t),$$

and $\zeta \in (0, 1), b > 0$. For the Zumo based MCAVs described here, $\zeta = 0.8, b = 70$ are chosen as appropriate values.

Merging scenario: There have been several approaches for automated vehicle merging as reported in Rios-Torres and Malikopoulos (2017a). In this paper, we consider the decentralized control approach described in Section 3 with

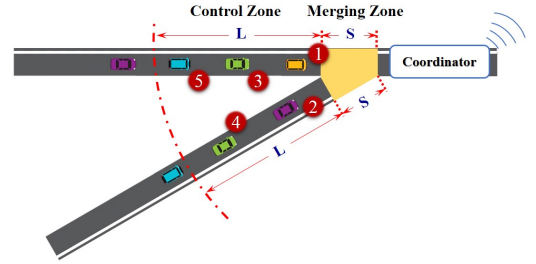


Fig. 6. Merging roads with connected and automated vehicles.

the Main Frame tracking the positions of each MCAV in order to determine when vehicles enter merging control regions. Practically a ROS service updates an ordered list as new cars enter a region and the boundaries of each region are indicated by a transition similarly to how transitions join road segments. Once inside a control region a virtual robot tracks the desired velocity profile exactly and reference tracking is used to mimic this behavior by the associated MCAV. The software is structured such that new control methods can be easily interchanged for comparison and testing highlighting another advantage of the UDSSC testbed.

Low level control: On-board encoders enable low-level control from inputs $u = [v, \omega]$, that are converted with two relationships,

$$v = R \frac{\dot{\phi}_R + \dot{\phi}_L}{2} \quad \omega = R \frac{\dot{\phi}_R - \dot{\phi}_L}{2}, \quad (3)$$

where ϕ_R, ϕ_L are the right and left wheels angular velocity respectively and R is wheel radius. High frequency control, however, results in noisy measurements due to low-resolution encoders. The Atmega 32U4 measures encoder pulses at a frequency of 2 kHz then smooths the velocity estimate by managing a running 25 measurement queue. Depending on the queue length, noise in the velocity measurement can be attenuated at the cost of increased settling time. A proportional controller adjusts the PWM duty cycle depending on the error between measured and desired velocity, saturating at $0.7\text{m/s} \pm 0.1\text{m/s}$ depending on transmission friction and slight mechanical variations between vehicles.

3. COORDINATION OF CONNECTED AND AUTOMATED VEHICLES

3.1 Modeling Framework

We consider a merging roadway (Fig. 6) consisting of main and secondary roads. The region that potential lateral collision between vehicles can occur is called *merging zone* and has a length of S . On each road, there is a *control zone* inside of which all vehicles can communicate with each other and with a coordinator. Note that the coordinator is not involved in any decision for any CAV and only enables communication of appropriate information among CAVs. The distance from the entry of the control zone to the entry of the merging zone is L . The value of L depends on the coordinator's communication range capability with

the CAVs, while $S < L$ is the physical length of a typical merging zone.

Let $N(t) \in \mathbb{N}$ be the number of CAVs inside the control zone at time $t \in \mathbb{R}^+$ and $\mathcal{N}(t) = \{1, \dots, N(t)\}$ be a queue which designates the order in which these vehicles will be entering the merging zone. Thus, letting t_i^m be the assigned time for vehicle i to enter the merging zone, we require that

$$t_i^m \geq t_{i-1}^m, \quad \forall i \in \mathcal{N}(t), \quad i > 1. \quad (4)$$

There are a number of ways to satisfy (4). For example, we may impose a strict First-in-First-Out (FIFO) queuing structure, where each vehicle must enter the merging zone in the same order it entered the control zone. More generally, however, t_i^m may be determined for each vehicle i at time t_i^0 when the vehicle enters the control zone and $\mathcal{N}(t_i^0) = \{1, \dots, i-1\}$. If $t_i^m > t_{i-1}^m$, then the order in the queue is preserved. If, on the other hand, there exists some $j \in \mathcal{N}(t_i^0)$, where $j < i-1$, such that $t_j^m > t_i^m > t_{j-1}^m$, then the order is updated so that CAV i is placed in the j th queue position. The policy through which the sequence is specified may be the result of a higher level optimization problem as long as the condition $t_i^m \geq t_{i-1}^m$ is preserved in between CAV arrival events at the control zone. In what follows, we will adopt a specific scheme for determining t_i^m (upon arrival of CAV i) based on our problem formulation, without affecting t_1^m, \dots, t_{i-1}^m , but we emphasize that our analysis is not restricted by the policy designating the order of the vehicles within the queue $\mathcal{N}(t)$.

We adopt the optimization framework proposed in Rios-Torres and Malikopoulos (2017b) for coordinating the merging of CAVs. The dynamics of each vehicle $i \in \mathcal{N}(t)$ are represented by a double integrator,

$$\dot{p}_i = v_i(t), \quad \dot{v}_i = u_i(t), \quad (5)$$

where $t \in \mathbb{R}^+$ denotes the time and $p_i(t) \in \mathcal{P}_i$, $v_i(t) \in \mathcal{V}_i$, and $u_i(t) \in \mathcal{U}_i$ denote position, speed and acceleration/deceleration (control input) of each vehicle $i \in \mathcal{N}(t)$ inside the control zone. Let $[p_i(t) \ v_i(t)]^T$ denote the state of each vehicle i , with initial value $[0 \ v_i^0]^T$. The state space $\mathcal{P}_i \times \mathcal{V}_i$ is closed with respect to the induced topology, thus, it is compact.

For any initial state $[p_i(t_i^0) \ v_i(t_i^0)]^T$, where t_i^0 is the time that the vehicle i enters the control zone, and every admissible control $u(t)$, the double integrator has a unique solution on some interval $[t_i^0, t_i^m]$, where t_i^m is the time that vehicle $i \in \mathcal{N}(t)$ enters the merging zone. In our framework we impose the following state and control constraints:

$$\begin{aligned} u_{i,min} &\leq u_i(t) \leq u_{i,max}, \quad \text{and} \\ 0 &\leq v_{min} \leq v_i(t) \leq v_{max}, \quad \forall t \in [t_i^0, t_i^m], \end{aligned} \quad (6)$$

where $u_{i,min}$, $u_{i,max}$ are the minimum and maximum control inputs (maximum deceleration/acceleration) for each vehicle $i \in \mathcal{N}(t)$, and v_{min} , v_{max} are the minimum and maximum speed limits respectively. For simplicity, in the rest of the paper we consider no vehicle diversity, and thus, we set $u_{i,min} = u_{min}$ and $u_{i,max} = u_{max}$.

For absence of any rear-end collision of two consecutive vehicles traveling on the same lane, the position of the preceding vehicle should be greater than or equal to the position of the following vehicle plus a safe distance $\delta(v_{ave}(t)) < S$, which is a function of the average speed of

the vehicles inside the control zone. Thus, we impose the following rear-end safety constraint

$$s_i(t) = p_k(t) - p_i(t) \geq \delta(v_{ave}(t)), \quad \forall t \in [t_i^0, t_i^m], \quad (7)$$

where k denotes the vehicle that is physically located ahead of i in the same lane, and $v_{ave}(t)$ is the average speed of the vehicles inside the control zone at time t .

Definition 1. Each CAV $i \in \mathcal{N}(t)$ belongs to at least one of the following two subsets of $\mathcal{N}(t)$ depending on its physical location inside the control zone: 1) $\mathcal{L}_i(t)$ contains all CAVs traveling on the same road and lane as vehicle i and 2) $\mathcal{C}_i(t)$ contains all CAVs traveling on a different road from i and can cause collision at the merging zone.

Definition 2. For each vehicle $i \in \mathcal{N}(t)$, we define the set Γ_i that includes only the positions along the lane where a lateral collision is possible, namely

$$\Gamma_i \triangleq \left\{ t \mid t \in [t_i^m, t_i^f] \right\}, \quad (8)$$

where t_i^f is the time that vehicle $i \in \mathcal{N}(t)$ exits the merging zone.

Consequently, to avoid a lateral collision for any two vehicles $i, j \in \mathcal{N}(t)$ on different roads, the following constraint should hold

$$\Gamma_i \cap \Gamma_j = \emptyset, \quad \forall t \in [t_i^m, t_i^f], \quad j \in \mathcal{C}_i(t). \quad (9)$$

The above constraint implies that only one vehicle at a time can be inside the merging zone. If the length of the merging is long, then this constraint may not be realistic since it results in dissipating space and capacity of the road. However, the constraint is not restrictive in the problem formulation and it can be modified appropriately.

In the modeling framework described above, we impose the following assumptions:

Assumption 1. The vehicles cruise inside the merging zone with an imposed speed limit, v_{srz} . This implies that for each vehicle i

$$t_i^f = t_i^m + \frac{S}{v_{srz}}. \quad (10)$$

This assumption is intended to enhance safety awareness, but it could be modified appropriately, if necessary.

3.2 Communication Structure of Connected and Automated Vehicles

We consider the problem of deriving the optimal control input (acceleration/deceleration) of each CAV inside the control zone (Fig. 6), under the hard safety constraints to avoid rear-end and lateral collision. By controlling the speed of the vehicles, the speed of queue built-up at the merging zone decreases, and thus the congestion recovery time is also reduced. The latter results in maximizing the throughput in the merging zone.

When a CAV i enters the control zone, it can communicate with the other CAVs that exist inside the control zone and with the coordinator. Note that the coordinator is not involved in any decision for any CAV and only enables communication of appropriate information among CAVs. The coordinator handles the information between the vehicles as follows. When a CAV reaches the control zone at some instant t , the coordinator assigns a *unique identity*

to each vehicle $i \in \mathcal{N}(t)$, which is a pair (i, j) , where $i = N(t) + 1$ is an integer representing the location of the vehicle in a FIFO queue $\mathcal{N}(t)$ and $j \in \{1, 2\}$ is an integer based on a one-to-one mapping from $\mathcal{L}_i(t)$ and $\mathcal{C}_i(t)$ onto $\{1, 2\}$. If the vehicles enter the control zone at the same, then the coordinator selects randomly their position in the queue.

Definition 3. For each CAV i entering the control zone, we define the *information set* $Y_i(t)$, which includes all information that each vehicle shares, as

$$Y_i(t) \triangleq \left\{ p_i(t), v_i(t), \mathcal{Q}, t_i^m \right\}, \forall t \in [t_i^0, t_i^m], \quad (11)$$

where $p_i(t), v_i(t)$ are the position and speed of CAV i inside the control zone, $\mathcal{Q} \in \{\mathcal{L}_i(t), \mathcal{C}_i(t)\}$ is the subset assigned to CAV i by the coordinator, and t_i^m is the time targeted for CAV i to enter the merging zone, whose evaluation is discussed next.

The time t_i^m that the vehicle i will be entering the merging zone is restricted by the imposing rear-end and lateral collision constraints. Therefore, to ensure that (7) and (9) are satisfied at t_i^m we impose the following conditions which depend on the subset that the vehicle $i - 1$ belongs to. If $i - 1 \in \mathcal{L}_i(t)$,

$$t_i^m = \max \left\{ \min \left\{ t_{i-1}^m + \frac{\delta(v_{ave}(t))}{v_{srz}}, \frac{L}{v_{min}} \right\}, \frac{L}{v_i(t_i^0)}, \frac{L}{v_{max}} \right\}, \quad (12)$$

and if $i - 1 \in \mathcal{C}_i(t)$,

$$t_i^m = \max \left\{ \min \left\{ t_{i-1}^m + \frac{S}{v_{srz}}, \frac{L}{v_{min}} \right\}, \frac{L}{v_i(t_i^0)}, \frac{L}{v_{max}} \right\}, \quad (13)$$

where v_{srz} , is the imposed speed inside the merging zone (Assumption 1), and $v_i(t_i^0)$ is the initial speed of vehicle i when it enters the control zone at t_i^0 . The conditions (12) and (13) ensures that the time t_i^m each vehicle i will be entering the merging zone is feasible and can be attained based on the imposed speed limits inside the control zone. In addition, for low traffic flow where vehicle $i - 1$ and i might be located far away from each other, there is no compelling reason for vehicle i to accelerate within the control zone to maintain a distance $\delta(v_{ave}(t))$ from vehicle $i - 1$, if $i - 1 \in \mathcal{L}_i(t)$, or a distance S if $i - 1 \in \mathcal{C}_i(t)$, at the time t_i^m that vehicle i enters the merging zone. Therefore, in such cases vehicle i can keep cruising within the control zone with the initial speed $v_i(t_i^0)$ that entered the control zone at t_i^0 .

The recursion is initialized when the first vehicle enters the control zone, i.e., it is assigned $i = 1$. In this case, t_1^m can be externally assigned as the desired exit time of this vehicle whose behavior is unconstrained. Thus the time t_1^m is fixed and available through $Y_1(t)$. The second vehicle will access $Y_1(t)$ to compute the times t_2^m . The third vehicle will access $Y_2(t)$ and the communication process will continue with the same fashion until the vehicle $N(t)$ in the queue access the $Y_{N(t)-1}(t)$.

3.3 Optimal Control Problem Formulation for Connected and Automated Vehicles

Since the coordinator is not involved in any decision on the vehicle coordination we can formulate $N(t)$ sequential

decentralized control problems that may be solved on-line:

$$\min_{u_i} \frac{1}{2} \int_{t_i^0}^{t_i^m} u_i^2(t) dt, \quad (14)$$

subject to : (5) and (6),

with initial and final conditions: $p_i(t_i^0) = 0, p_i(t_i^m) = L, t_i^0, v_i(t_i^0), t_i^m$, and $v_i(t_i^m) = v_{srz}$. In the problem formulation above, we have omitted the rear end (7) and lateral (9) collision safety constraints. As mentioned earlier, (9) implicitly handled by the selection of t_i^m in (13). Eq. (7) is omitted because it has been shown Malikopoulos et al. (2017) that the solution of (14) guarantees that this constraint holds throughout $[t_i^0, t_i^m]$. Thus, (14) is a simpler problem to solve on-line.

For the analytical solution and real-time implementation of the control problem (14), we apply Hamiltonian analysis. In our analysis, we consider that when the vehicles enter the control zone, none of the constraints are active. To address this problem, the constrained and unconstrained arcs need to be pieced together to satisfy the Euler-Lagrange equations and necessary condition of optimality. The analytical solution of (14) without considering state and control constraints was presented in Ntousakis et al. (2016); Rios-Torres et al. (2015); Rios-Torres and Malikopoulos (2017b) for coordinating in real time CAVs at highway on-ramps and Zhang et al. (2016) at two adjacent intersections. When the state and control constraints are not active, the optimal control input (acceleration/deceleration) as a function of time is given by

$$u_i^*(t) = a_i t + b_i, \quad (15)$$

and the optimal speed and position for each vehicle are

$$v_i^*(t) = \frac{1}{2} a_i t^2 + b_i t + c_i \quad (16)$$

$$p_i^*(t) = \frac{1}{6} a_i t^3 + \frac{1}{2} b_i t^2 + c_i t + d_i, \quad (17)$$

where a_i, b_i, c_i and d_i are constants of integration. These constants can be computed by using the initial and final conditions. Since we seek to derive the optimal control (15) in real time, we can designate initial values $p_i(t_i^0)$ and $v_i(t_i^0)$, and initial time, t_i^0 , to be the current values of the states $p_i(t)$ and $v_i(t)$ and time t , where $t_i^0 \leq t \leq t_i^m$. Similar results to (15)-(16) can be obtained when the state and control constraints become active Malikopoulos et al. (2017).

4. EXPERIMENTAL RESULTS

To evaluate the effectiveness of the efficiency of the proposed approach, a total number of 10 MCAVs are set up in a merging scenario [video available in IDS (2017)]. Five MCAVs cruise on the main road in UDSSC, while the other five MCAVs cruise on the secondary road with the intention to merge into the main road (as shown in Fig. 7).

We considered the following two scenarios: 1) all MCAVs will be controlled by the decentralized control algorithm; and 2) all MCAVs will behave based on a simple lane following model, based on which the MCAVs cruising on the secondary road will have to yield to MCAVs of the main road to avoid potential lateral collision inside the merging zone (baseline scenario).



Fig. 7. Aerial view of the actual control and merging regions.

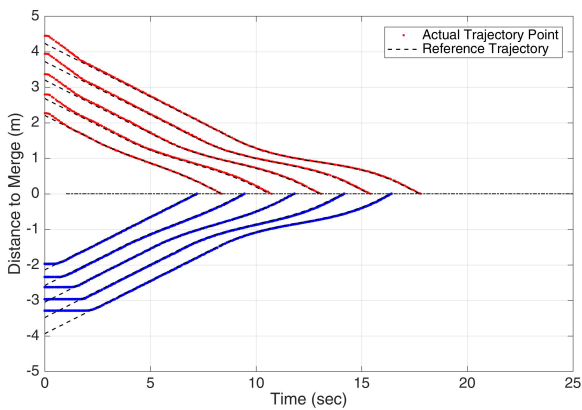


Fig. 8. Vehicle trajectory under optimal control.

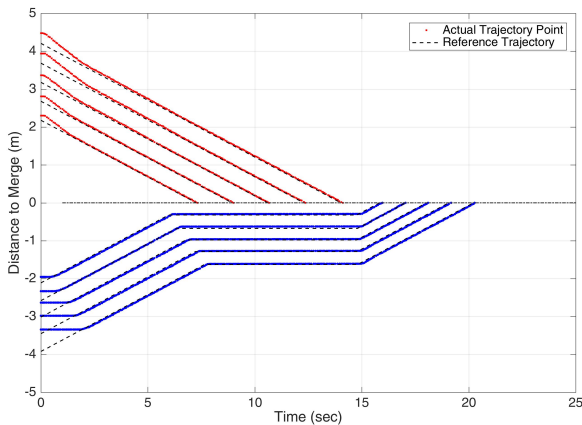


Fig. 9. Vehicle trajectory without optimal control.

Vehicle Position Trajectory: The position trajectories of the MCAVs under the first scenario are illustrated in Fig. 8. The dashed line represents the reference trajectory for each vehicle commanded by the control algorithm, while a dense scatter plot represents the point measured along the actual trajectory achieved by each MCAV. To separate the MCAVs on two roads, the trajectories are flipped over Y-axis. Thus, in Fig. 8, the red dots stand for the trajectory points of the MCAVs of main road, and the blue dots stand for the trajectory points of the MCAVs of the secondary roads. The MCAVs are able to follow

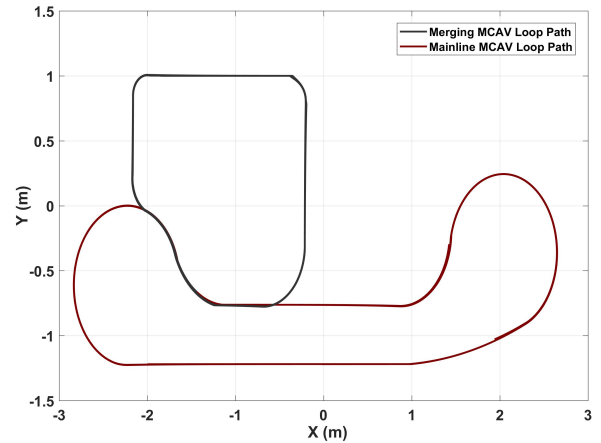


Fig. 10. Driving loops for battery level evaluation.

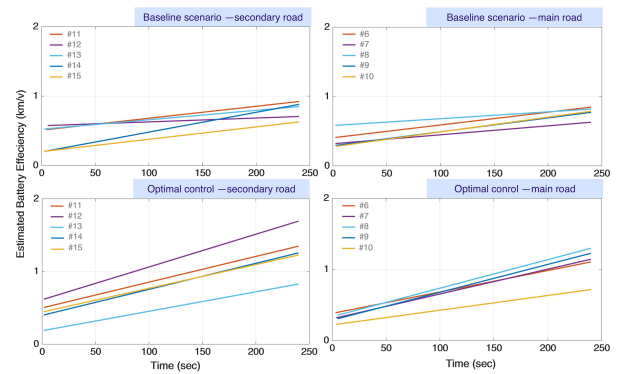


Fig. 11. Battery efficiency over time.

the optimal trajectory and manage to merge successfully without stop-and-go driving with only marginal errors. The position trajectories of the MCAVs cruising without the optimal control (baseline scenario) are shown in Fig. 9. Since the gaps between the mainline cars are not large enough for the merging cars to safely merge into the roadway, the merging cars need to stop until all the leading mainline vehicles traverse the merging zone, resulting in a queue built up on the merging roadway segment. For comparison, the merging maneuver for all the ten cars is completed in 16.5 sec with the optimal control algorithm, whereas it takes 20.3 sec for all the cars to pass the merging point (i.e., an 18.7% travel time savings is achieved with the proposed optimal control algorithm).

State-of-Charge of the Battery: To quantify the benefits of vehicle coordination, we compare the battery state of charge (SOC) of MCAVs. Under both scenarios, the MCAVs loop around the merging zone following a pre-defined trajectory as shown in Fig. 10. SOC is recorded for MCAVs under the two scenarios are illustrated in Fig. 11. From the final SOC of each MCAV (Fig. 12), it is clear that coordination of MCAVs improves the efficiency of the battery in the merging scenario of MCAVs due to the elimination of the stop-and-go driving.

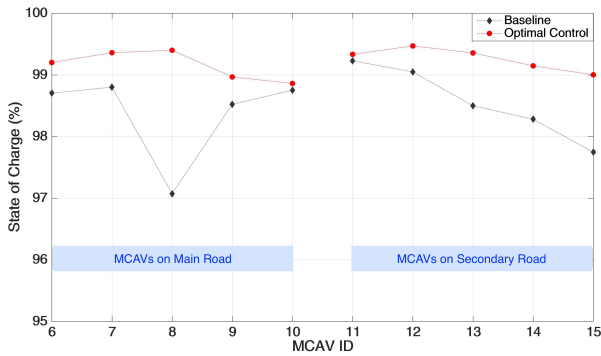


Fig. 12. Final state of charge of the battery for each robotic car.

5. CONCLUDING REMARKS

UDSSC is a small-scale “smart” city that can replicate real-world traffic scenarios in a small and controlled environment. This testbed can be an effective way to visualize the concepts developed in real world traffic scenarios using CAVs in a quick, safe and affordable way. The UDSSC helps bridge the gap between theory and practical implementation by providing a means of simultaneously testing as many as 35 MCAVs. We used UDSSC to validate experimentally a control framework reported in Rios-Torres and Malikopoulos (2017b) for coordination CAVs. The results demonstrate that coordination of CAVs can improve the battery efficiency due to elimination of the stop-and-go driving.

ACKNOWLEDGEMENTS

The authors would like to acknowledge the contributions of Caili Li (University of Delaware) for the assistance in the software architecture, Yue Feng (University of Delaware) for establishing a robust communication network and user interface for connecting MCAVs, Grace Gong (Wilmington Charter High School) for vehicle design, and Abhinav Ratnagiri (Concord High School) for constructing a low level serial communication between the Raspberry Pi 3 and Zumo.

REFERENCES

Alonso, J., Milanés, V., Pérez, J., Onieva, E., González, C., and de Pedro, T. (2011). Autonomous vehicle control systems for safe crossroads. *Transportation Research Part C: Emerging Technologies*, 19(6), 1095–1110.

Antoniotti, M., Deshpande, A., and Girault, A. (1997). Microsimulation analysis of automated vehicles on multiple merge junction highways. *IEEE International Conference in Systems, Man, and Cybernetics*, 839–844.

Dresner, K. and Stone, P. (2004). Multiagent traffic management: a reservation-based intersection control mechanism. In *Proceedings of the Third International Joint Conference on Autonomous Agents and Multiagent Systems*, 530–537.

Giuseppe, Oriolo, D.L.A. and Vendittelli, M. (2002). Wmr control via dynamic feedback linearization: Design, implementation, and experimental validation. *IEEE Transactions on Control Systems Technology*, 10(6), 835–852.

IDS(2017) (????).

Kachroo, P. and Li, Z. (1997). Vehicle merging control design for an automated highway system. In *Proceedings of Conference on Intelligent Transportation Systems*, 224–229.

Lu, X.Y., Tan, H.S., Shladover, S.E., and Hedrick, J.K. (2000). Implementation of longitudinal control algorithm for vehicle merging. *Proceedings of the AVEC 2000*.

Malikopoulos, A.A. and Aguilar, J.P. (2013). An Optimization Framework for Driver Feedback Systems. *IEEE Transactions on Intelligent Transportation Systems*, 14(2), 955–964. doi:10.1109/TITS.2013.2248058.

Malikopoulos, A.A., Cassandras, C.G., and Zhang, Y. (2017). A decentralized energy-optimal control framework for connected automated vehicles at signal-free intersections. *arXiv:1602.03786 - (provisionally accepted)*.

Margiotta, R. and Snyder, D. (2011). An agency guide on how to establish localized congestion mitigation programs. Technical report, U.S. Department of Transportation. Federal Highway Administration.

Milanés, V., Pérez, J., and Onieva, E. (2010). Controller for Urban Intersections Based on Wireless Communications and Fuzzy Logic. *IEEE Transactions on Intelligent Transportation Systems*, 11(1), 243–248. doi: 10.1109/TITS.2009.2036595.

Ntousakis, I.A., Nikolos, I.K., and Papageorgiou, M. (2016). Optimal vehicle trajectory planning in the context of cooperative merging on highways. *Transportation Research Part C: Emerging Technologies*, 71, 464–488.

Ran, B., Leight, S., and Chang, B. (1999). A microscopic simulation model for merging control on a dedicated-lane automated highway system. *Transportation Research Part C: Emerging Technologies*, 7(6), 369–388.

Rios-Torres, J., Malikopoulos, A.A., and Pisu, P. (2015). Online Optimal Control of Connected Vehicles for Efficient Traffic Flow at Merging Roads. In *2015 IEEE 18th International Conference on Intelligent Transportation Systems*, 2432 – 2437.

Rios-Torres, J. and Malikopoulos, A.A. (2017a). A Survey on Coordination of Connected and Automated Vehicles at Intersections and Merging at Highway On-Ramps. *IEEE Transactions on Intelligent Transportation Systems*, 18(5), 1066–1077.

Rios-Torres, J. and Malikopoulos, A.A. (2017b). Automated and Cooperative Vehicle Merging at Highway On-Ramps. *IEEE Transactions on Intelligent Transportation Systems*, 18(4), 780–789.

Schrank, B., Eisele, B., Lomax, T., and Bak, J. (2015). 2015 Urban Mobility Scorecard. Technical report, Texas A& M Transportation Institute.

VanMiddlesworth, M., Dresner, K., and Stone, P. (2008). Replacing the stop sign: unmanaged intersection control for autonomous vehicles. In *Proc. 5th Workshop Agents Traffic Transport. Multiagent Syst.*, 94–101.

Zhang, Y., Malikopoulos, A.A., and Cassandras, C.G. (2016). Optimal control and coordination of connected and automated vehicles at urban traffic intersections. In *Proceedings of the 2016 American Control Conference*, 5014–5019.